J. Fluid Mech. (1988), *vol.* 195, *pp.* 175–200
Printed in Great Britain

Soret separation in a quasi-vertical cylinder

By D. HENRY† AND B. ROUX‡

† Laboratoire de Mécanique des Fluides, Ecole Centrale de Lyon, BP163, F-69131 Ecully cedex, France

‡ Institut de Mécanique des Fluides, UM 34 du CNRS, F-13003 Marseille, France

(Received 11 March 1987 and in revised form 9 February 1988)

This paper deals with the Soret separation of a binary mixture in a cylinder subjected to an axial temperature gradient. The study is connected to an experiment designed to measure the Soret coefficient of an AgI–KI mixture corresponding to a moderate Prandtl number ($Pr = 0.6$) and a high Schmidt number ($Sc = 60$). In such an experiment the species separation is often hidden by a mixing effect due to the buoyancy-driven convection generated by a horizontal temperature gradient induced by some defect of the heating system. Here, such a defect is simulated by a slight misorientation of the cell with respect to the vertical; a small inclination ($\gamma = 1°$) of the cell has been considered, but the results can be generalized for any other small γ. For situations corresponding to a top heating and a positive Soret parameter, S, two quite different regimes have been exhibited depending on the value of S. For moderate S, the induced solutal buoyancy balances the imposed thermal buoyancy, slowing down the flow and giving a good separation rate. For small S this balance does not exist (except in the centre), leading to a remixing of the species and thus to poor separation (the separation would be still worse for negative S). The smaller the (positive) Soret parameter is, the smaller the cell misorientation γ has to be to allow a good separation rate.

1. Introduction

Several papers have been devoted to the experimental determination of the Soret coefficient of a binary mixture and various techniques have been proposed for it. In most of these experiments the mixture is placed in a container subjected to a temperature gradient, generally vertical. The top and the bottom of such a container have to be perfectly isothermal and horizontal in order to avoid a horizontal temperature gradient, which always generates convection and may cause some 'undesirable' remixing.

The separation between the species that results from the Soret effect is measured by different kinds of techniques (direct concentration measurement, optical or electrical measurements, etc.). The results reported in the literature show large discrepancies (see Velarde & Schechter 1971), and even opposite signs of the Soret coefficient. Thomaes (1975) mentions that in contrast to the predictions of kinetic, thermodynamic and statistical theories, only a few systems have been found to have negative S. Most of these discrepancies are attributed to convection (De Groot 1947; Agar & Turner 1960; Dulieu, Chanu & Walch 1981), which is difficult to suppress, particularly when a large temperature gradient must be imposed.

Various apparatuses have been designed to limit the perturbating effect of such convection by using a porous disk (Sundheim & Kellner 1965) or numerous thin-walled tubes (Longree, Legros & Thomaes 1980), or by confining the convection to

a small part of the cell in order to neglect it (Legros, Van Hook & Thomaes 1968; Legros, Rasse & Thomaes 1970; J. Richter & H. Valenta 1986, private communication).

As the convection is present in many other experiments, a lot of papers have been devoted to it, mainly through a stability analysis of the steady state of a mixture subjected to a vertical temperature gradient. Most of them concern the linear stability in horizontal (non-confined) layers (Platten & Chavepeyer 1972; Schechter, Prigogine & Hamm 1972; Schechter, Velarde & Platten 1974; Chock & Li 1975; Gutkowicz-Krusin, Collins & Ross 1979) and more recently in confined vertical cylinders (Crespo & Velarde 1982; G. R. Hardin & R. L. Sani 1983, private communication; Henry & Roux 1983; Hardin *et al.* 1988). A nonlinear stability analysis has also been done for horizontal layers by Platten & Chavepeyer (1976, 1977), and for confined vertical cylinders by G. R. Hardin & R. L. Sani (1986, private communication).

Furthermore, experiments have been performed to analyse the onset of convection and the flow structure of a mixture subjected to the Soret effect: Shirtcliffe (1969) for salt water, Verhoeven (1969) for mercury, Hurle & Jakeman (1971) for water–methanol, Caldwell (1973) for aqueous salt solutions, Olson & Rosenberger (1979) and Abernathey & Rosenberger (1981) for gases. Caldwell (1973) suggested measuring negative thermal diffusion coefficients by observing the onset of thermohaline convection.

Soret-driven thermosolutal convection has been suggested by Hurle & Jakeman (1969) to have an effect even in nominally pure liquids (e.g. in the experiments of Harp & Hurle 1968 and Verhoeven 1969). It is also found to affect crystallization of single crystals grown from melts containing a solute (Hurle & Jakeman 1971). This last assertion is confirmed by Chien & Mattes (1983) in a study of thermal (Soret) diffusion in the liquid-phase epitaxial growth of binary III–V compounds, like GaAs.

Most of the previous theoretical studies have been devoted to the stability of stratified layers at rest in the following three cases: a container heated from below for positive and negative Soret parameter, S, and from above for negative S. A direct simulation of supercritical situations also exists for the first and the third cases (Henry & Roux 1987*a*). The second case would correspond to unsteady flows; it has so far only been numerically simulated for a simpler geometry (a rectangular container at $S = -0.01$, $Pr = 10$, $Sc = 1000$ and $Ra = 3000$) by Platten & Legros (1984).

In the present paper only layers with a stable stratification in a cylinder heated from above are analysed, with emphasis on positive-S cases. (A few negative S cases also are considered.) The primary goal is to show the difficulties inherent in the measurement of the Soret coefficient of a binary mixture, mainly for fluids corresponding to high values of the Schmidt number, $Sc = \nu/D$, like the molten salts or liquid metals. As the experiments require strong temperature differences in order to achieve significant species separation, the smallest geometrical defect products a significant non-vertical temperature gradient and generates a buoyancy-driven flow which induces a remixing of the species and limits the Soret separation. To simulate such a defect, we consider the case of small cell-inclinations γ (quasi-vertical cylinders) and analyse the flow structure and the remixing rate of a binary mixture for such small inclinations. We shall mainly consider the case $\gamma = 1°$.

In view of these difficulties for experiments at the ground level, several experiments have been planned in a space environment in order to reduce the natural convection

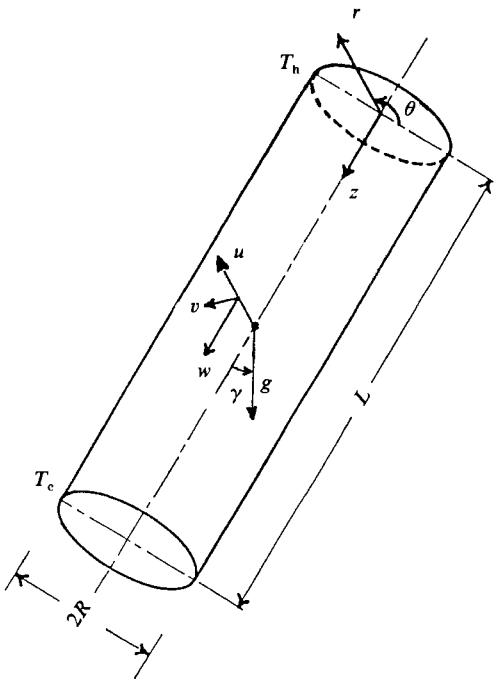

FIGURE 1. Differentially heated cylinder: definition sketch for dimensions, location coordinates and velocity components.

(Bert *et al.* 1984; Bert, Moussa & Dupuy 1987; Malmejac & Praizey 1984; Praizey 1987). In fact in a space environment the gravity is only reduced by a factor of 10^3–10^4, and the convection is not always negligible; in addition, the orientation of the (residual) gravity vector with respect to the container is generally not known in advance. Two previous studies (Henry & Roux 1986, 1987*a*) related to experiments performed in space (Bert *et al.* 1987) have been devoted to the remixing process in horizontal and inclined cylinders for low-g conditions, i.e. for small Grashof numbers ($0 \leqslant Gr \leqslant 10$) for which the flow is typically of a 'conducting' type (the isotherms being only slightly distorted by the buoyancy-driven flow). For such moderate convection a reinterpretation of the experiments is possible through the calculated remixing rate. A secondary goal of the present study is to enable a comparison between the remixing rate in a cylindrical cell at a small inclination γ (with respect to the gravity vector g_0; see figure 1) in ground situations, and at any γ in low-g situations ($g \sim 10^{-3} g_0$).

A more general aim of this study is to give new insights into double-diffusive convection when a direct coupling exists between the two diffusive processes. Following the argument given by Hurle & Jakeman (1969) about the Soret effect, even in normally pure liquid, this study could be relevant to crystal-growth techniques involving a vertical temperature gradient (such as the Bridgman technique). Soret diffusion was found by Hurle & Jakeman (1969) to cause oscillations in the case of unstable stratification; in our case, i.e. for stable stratification, it could generate a flow and thus a macrosegregation near the solidification front.

We mainly consider values of S in the range $0 \leqslant S \leqslant 0.673$. The aspect ratio of the cylinder $A = L/R$ (L length, R radius) is taken to equal 3. The values of Grashof

number are taken in the range $482 \leqslant Gr \leqslant 4820$. The study is limited to the case of conducting walls, as we expect that the isotherms will not be too much distorted by the flow as long as γ is small.

Some of the results discussed herein were presented in Henry & Roux (1987*b*). This work is a summary of one part of the thesis of Henry (1986).

2. Hypothesis and mathematical description of the model

As in the usual simplified Boussinesq assumptions, physical properties (kinematic viscosity ν, diffusivity κ, and total density ρ) are assumed to be constant, except in the buoyancy term where $\bar{\rho}$ is taken as a linear function of the temperature $\bar{T}$ and of the mass fraction $\bar{X}$ (of the heavier component):

$$\bar{\rho} = \bar{\rho}_0[1-\alpha(\bar{T}-\bar{T}_0)+\beta(\bar{X}-\bar{X}_0)], \tag{1}$$

where α and β are respectively the thermal and solute expansion coefficients, and an overbar denotes a dimensional quantity.

Accounting for the thermal-diffusion (or Soret) effect, the usual phenomenological equation relating the mass flux, $\boldsymbol{J}_X$, to the thermal and solutal gradients is

$$\boldsymbol{J}_X = -\bar{\rho}D'\bar{X}(1-\bar{X})\,\boldsymbol{\nabla}\bar{T}-\bar{\rho}D\boldsymbol{\nabla}\bar{X},$$

where D and D' are respectively the solute and thermal diffusion coefficients.

The walls are assumed to be rigid and impervious; both ends of the cylinder are kept at a fixed temperature ($\bar{T}_c$ and $\bar{T}_h$). Along the conducting lateral walls the temperature varies linearly.

We use the same scaling factors as in a previous paper (Henry & Roux 1986), i.e. R and $Gr\,\nu/R$, for length and velocity. The reference quantities for temperature and mass fraction are

$$\bar{T}_{\text{ref}} = \frac{\bar{T}_h-\bar{T}_c}{A}, \quad \bar{X}_{\text{ref}} = \frac{D'\bar{X}_0(1-\bar{X}_0)(\bar{T}_h-\bar{T}_c)}{DA},$$

with the overbar indicating a dimensional quantity. The dimensionless temperature and mass-fraction are taken as

$$T = \frac{\bar{T}-\bar{T}_0}{\bar{T}_{\text{ref}}}, \quad X = \frac{\bar{X}-\bar{X}_0}{\bar{X}_{\text{ref}}}$$

where $\bar{X}_0$ is the initial mass-fraction at the mean temperature $\bar{T}_0 = \frac{1}{2}(\bar{T}_h+\bar{T}_c)$. The mass fraction is non-dimensionalized with a value corresponding to the rate of separation per unit length in the 'perfect' Soret case (without motion), giving the values $+\frac{1}{2}A$ and $-\frac{1}{2}A$ at, respectively, the cold and warm ends. The rate of separation, $\partial X/\partial z$, is then equal to 1.

We seek steady-state solutions, but in order to accelerate the convergence of our iterative algorithm, a false transient technique (see Leong & de Vahl Davis 1979) is used for the transport equations in $\boldsymbol{Z}$, T and X, with different timescaling factors (respectively, R^2/ν, R^2/κ and R^2/D). The following dimensionless parameters previously considered by Henry & Roux (1986) are used: Soret parameter and Prandtl, (thermal) Grashof and Schmidt numbers, respectively defined as

$$S = \frac{\bar{X}_0(1-\bar{X}_0)\beta D'}{\alpha D}, \quad Pr = \frac{\nu}{\kappa}, \quad Gr = \frac{\alpha g R^3(\bar{T}_h-\bar{T}_c)}{\nu^2 A}, \quad Sc = \frac{\nu}{D}.$$

Thus, from mass, momentum and energy balances (see Leong & de Vahl Davies 1979 and Henry & Roux 1986) we obtain the following three-dimensional system expressed in terms of the vorticity vector $\boldsymbol{Z}(Z_1, Z_2, Z_3), T, X$ and the velocity vector $\boldsymbol{V}(u, v, w)$:

$$\frac{\partial \boldsymbol{Z}}{\partial t} = Gr\,\boldsymbol{\nabla} \times (\boldsymbol{V} \times \boldsymbol{Z}) - \boldsymbol{\nabla} \times (\tilde{g}T) + S\boldsymbol{\nabla} \times (\tilde{g}X) - \boldsymbol{\nabla} \times (\boldsymbol{\nabla} \times \boldsymbol{Z}), \tag{2}$$

$$\frac{\partial T}{\partial t} = -Gr\,Pr\,\boldsymbol{\nabla} \cdot (T\boldsymbol{V}) + \nabla^2 T, \tag{3}$$

$$\frac{\partial X}{\partial t} = -Gr\,Sc\,\boldsymbol{\nabla} \cdot (X\boldsymbol{V}) + \nabla^2 T + \nabla^2 X, \tag{4}$$

$$\nabla^2 \boldsymbol{V} = -\boldsymbol{\nabla} \times \boldsymbol{Z}. \tag{5}$$

The associated boundary conditions are

$$u = v = w = 0, \quad (\boldsymbol{J}_X)_n = (\boldsymbol{\nabla} T + \boldsymbol{\nabla} X)_n = 0$$

on the boundaries (rigid and not reactive);

$$Z_1 = -\frac{\partial v}{\partial z}, \quad Z_2 = \frac{\partial u}{\partial z}, \quad Z_3 = 0 \quad \text{at } z = 0, \quad z = A;$$

$$Z_1 = 0, \quad Z_2 = -\frac{\partial w}{\partial r}, \quad Z_3 = \frac{\partial v}{\partial r} \quad \text{at } r = 1;$$

$$T_{(z=0)} = \tfrac{1}{2}A, \quad T_{(z=A)} = -\tfrac{1}{2}A; \quad T = 0 \quad \text{at } r = 1$$

(perfectly conducting).

The system (2)–(5) involves the classical condition, $\boldsymbol{\nabla} \cdot \boldsymbol{V} = 0$, corresponding to the Boussinesq assumption (quasi-incompressible fluid). The validity of such an assumption has been discussed by Henry & Roux (1987*a*).

The finite-difference method used to solve the system (2)–(5) is basically the one developed by Leong & de Vahl Davis (1979); its implementation on a CRAY computer is given in previous papers (Smutek *et al.* 1984; Henry & Roux 1986). The code is used in its 'false-transient' version, which is well suited and efficient for steady-state situations; but of course it would not converge if the flow was unsteady (the code would then have to be run in its fully transient version). All the results presented in this study correspond to steady-state flows; they are obtained with the convergence criterion used by Henry & Roux (1986) (here, $\epsilon = 10^{-3}$) and with, respectively, 33, 9 and 32 mesh points in the longitudinal (z), radial (r) and azimuthal (θ) directions.

3. General results and comments

We look at the absolute value of the mean mass fraction, $X_m(k)$, in a z-plane at various mesh-point positions k ($k = 1$ corresponds to the hot endwall and $k = 33$ to the cold endwall). The global separation will be given by $X_m(1)$, or by $X_{\text{bot}} = X_m(1)/\frac{1}{2}A$ which is a 'measure' of the ratio of the effective and 'perfect' Soret separation between the two endwalls. We mainly analyse the numerical results through velocity, isotherm and iso-mass-fraction fields in the vertical symmetry plane (denoted as the V-plane). For a quantitative interpretation of isotherm and iso-mass-fraction fields we need the position of the zero isocontour (it

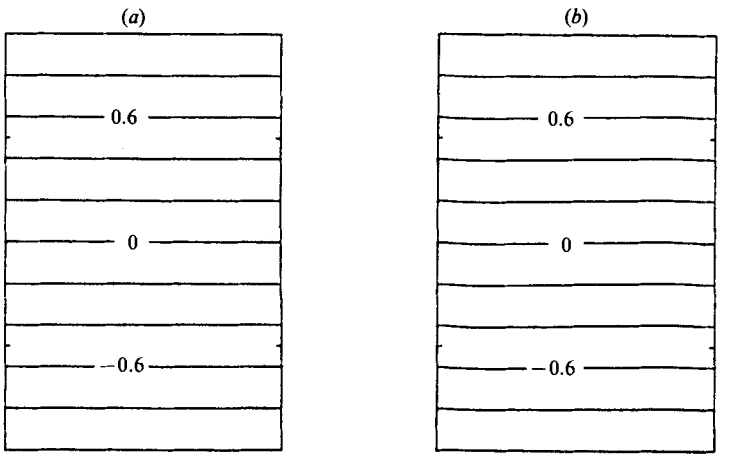

FIGURE 2. Isotherm patterns in the V-plane: (*a*) $Gr = 482$ and $S = 0.673$; (*b*) $Gr = 4820$ and $S = 0$.

is the one passing through the centre) and the isocontours spacing, DX, that is given for each graph (or DT which is always taken as 0.2). Together with $\bar{V}$, we shall use $\tilde{V} = \bar{V}/(\nu/R)$; e.g. we will consider the maximum of the velocity in the V-plane, $\tilde{V}_{\max}$.

With respect to the signification of the limiting case $S = 0$, we must point out that this case involves two situations depending on whether β equals zero or not. When S goes to zero with β, $\bar{X}_{\text{ref}}$ remains finite, thus indicating that a separation exists ($\bar{X} \neq \bar{X}_0$) even for $S = 0$, but this separation does not affect the motion (no solutal buoyancy forces). In the second case, where β is finite, we have $\bar{X}_{\text{ref}} = S\alpha(\bar{T}_{\text{h}} - \bar{T}_{\text{c}})/(\beta A)$; thus $\bar{X}_{\text{ref}}$ goes to zero with S, but X still has a finite value if the separation vanishes ($\bar{X}$ tends to X_0) and can be interpreted as

$$X = \frac{\bar{X} - \bar{X}_0}{\bar{X}_{\text{ref}}} = \frac{(\bar{X} - \bar{X}_0)\beta A}{S\alpha(\bar{T}_{\text{h}} - \bar{T}_{\text{c}})} = \frac{(\bar{X}_S)_{S=0}\beta A}{\alpha(\bar{T}_{\text{h}} - \bar{T}_{\text{c}})};$$

thus X represents the derivative ($\bar{X}_S$) at $S = 0$, from which the actual separation can be obtained for any sufficiently small S.

The temperature fields drawn in the V-plane are given in figures 2(*a*) and 2(*b*) for two extreme convective situations: $Gr = 482$ for $S = 0.673$ and $Gr = 4820$ for $S = 0$. In the first case, characterized by a higher value of S, figure 2(*a*) shows that the isotherms remain practically parallel to the endwalls. In the second example (see figure 2*b*), the isotherms appear to be slightly distorted by the flow, but this is enough to have a significant effect on the convective flow.

In figures 3 and 4 respectively we plot $\tilde{V}_{\max}$ and X_{bot} versus S, for three values of Gr: 482, 1446 and 4820. These figures show two regimes; one corresponding to small values of S ($0 \leqslant S \leqslant 0.03$) for which $\tilde{V}_{\max}$ reaches high values (increasing with Gr) and the other corresponding to higher S ($S \geqslant 0.05$) for which $\tilde{V}_{\max}$ remains small and the separation is good (X_{bot} close to 1) for any value of Gr. We shall separately analyse these two regimes in detail.

For a better understanding of the physical mechanisms, it is useful to consider the

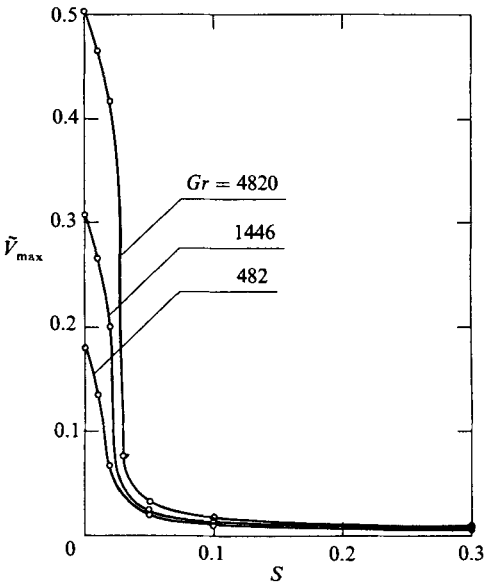

FIGURE 3. Maximum of the velocity *vs.* Soret parameter, for various Gr.

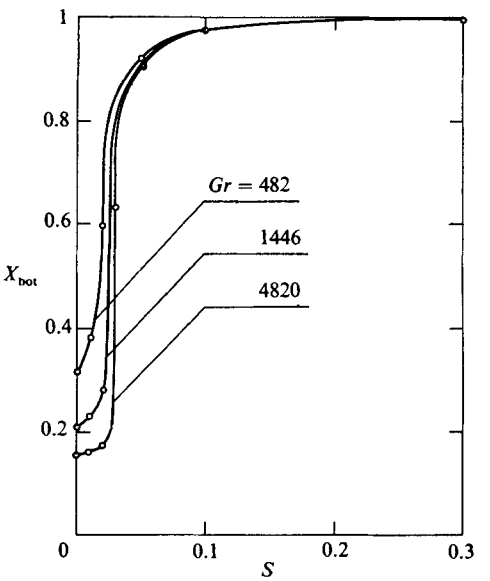

FIGURE 4. Global species separation, X_{bot} *vs.* Soret parameter, for various Gr.

expressions for the two contributions (thermal and solutal) of the buoyancy forces, F_T and F_X, in the V-plane. These expressions can be written as follows for $\gamma = 1°$:

$$F_T = -T_z \sin(1°) + T_r \cos(1°) \tag{6}$$

and

$$F_X = S[X_z \sin(1°) - X_r \cos(1°)]. \tag{7}$$

It is also interesting to consider the angle α_X of the zero-mass-fraction contour with the vertical (or the angle β_X so that $\alpha_X = \beta_X + 90° - \gamma$). Similarly, for the isotherm $T = 0$, we can consider the angles α_T and β_T. In that case, we have

$$F_X = SX_n \cos(\alpha_X) = -SX_n \sin(\beta_X - \gamma) \tag{8}$$

and

$$F_T = -T_n \cos(\alpha_T) = T_n \sin(\beta_T - \gamma), \tag{9}$$

where the subscript n denotes a derivative in the direction normal to the zero-X or zero-T contour. Thus, the sign of F_i changes when $\alpha_i \geqslant 90°$ (or $\beta_i \geqslant \gamma$), i.e. when the zero-X or zero-T contour overpass the horizontal. As $S > 0$ and $T_n < 0$ ($T_n \sim -1$), F_X acts in the same way as F_T when the mass-fraction field is slightly distorted ($\beta_X < \gamma$), but acts in an opposite way as soon as $\beta_X \geqslant \gamma$ (i.e. here, for a deformation of the mass-fraction contours just higher than 1°).

For $S \geqslant 0.05$, as T_z is close to -1 and T_r is close to 0, we have

$$F_T = \sin(1°). \tag{10}$$

For small S a slight isotherm deformation, β_T, is sufficient to slow down the flow or stop it (for $\beta_T = \gamma$).

4. Small Soret parameter ($0 \leqslant S \leqslant 0.03$)

The velocity fields presented in figure 5 show that the fluid motion in the V-plane corresponds to a single roll flowing parallel to the lateral wall and recirculating at the endwalls. When Gr increases, the flow seems to concentrate nearer the lateral wall, leaving a large area of dead fluid in the centre. The flow intensity given by $\tilde{V}_{\max}$ is not proportional to Gr (even for $S = 0$), in contrast to the case of low Gr considered in our previous studies.

These characteristics suggest that we have a balance between buoyancy and inertia forces, that would give a variation of $\tilde{V}_{\max}$ as $Gr^{\frac{1}{2}}$, for $S = 0$. In fact, the exponent of Gr in the expression of $\tilde{V}_{\max}$ is clearly found to be less than $\frac{1}{2}$. In addition, a direct comparison between the different terms of the θ-projection of equation (2), in the V-plane, for $S = 0$, indicates that the balance in this plane is realized between buoyancy and viscous forces, which is more consistent with the fact that such situations are only slightly convective.

Thus the zero velocity in the centre is mainly due to the vanishing of buoyancy forces. For $S = 0$, where only the thermal contribution plays a role, we can verify that the isotherm deformation in the centre, β_T, is close to 1°. This deformation ($\beta_T = 1°$ in the centre) exists over a longer r-distance when Gr increases. Near the lateral walls, the conducting boundary conditions involve isotherm deformation in the reverse sense and favour the motion. In fact, the main motion is generated there, and cannot correspond to a usual 'core-driven' flow.

Although the cylinder is not long ($A = 3$), there is an area in the central region where the flow is uniform (z-independent). This domain corresponds, in figure 6, to the portion of the $|X_m(z)|/\frac{1}{2}A$ curves having a constant slope; however, iso-mass-fraction contours are strongly distorted by the motion, as shown in figure 7, for the V-plane. These deformations affect the entire cylinder as shown through the three-dimensional representation of the zero-mass-fraction contour, plotted in figure 8 for $S = 0$ and in figure 9 for $S = 0.02$. The deformations increase with Gr, being already important at $Gr = 482$ for $S = 0$. In all cases, they are associated with a very poor separation rate, as observed in figure 6.

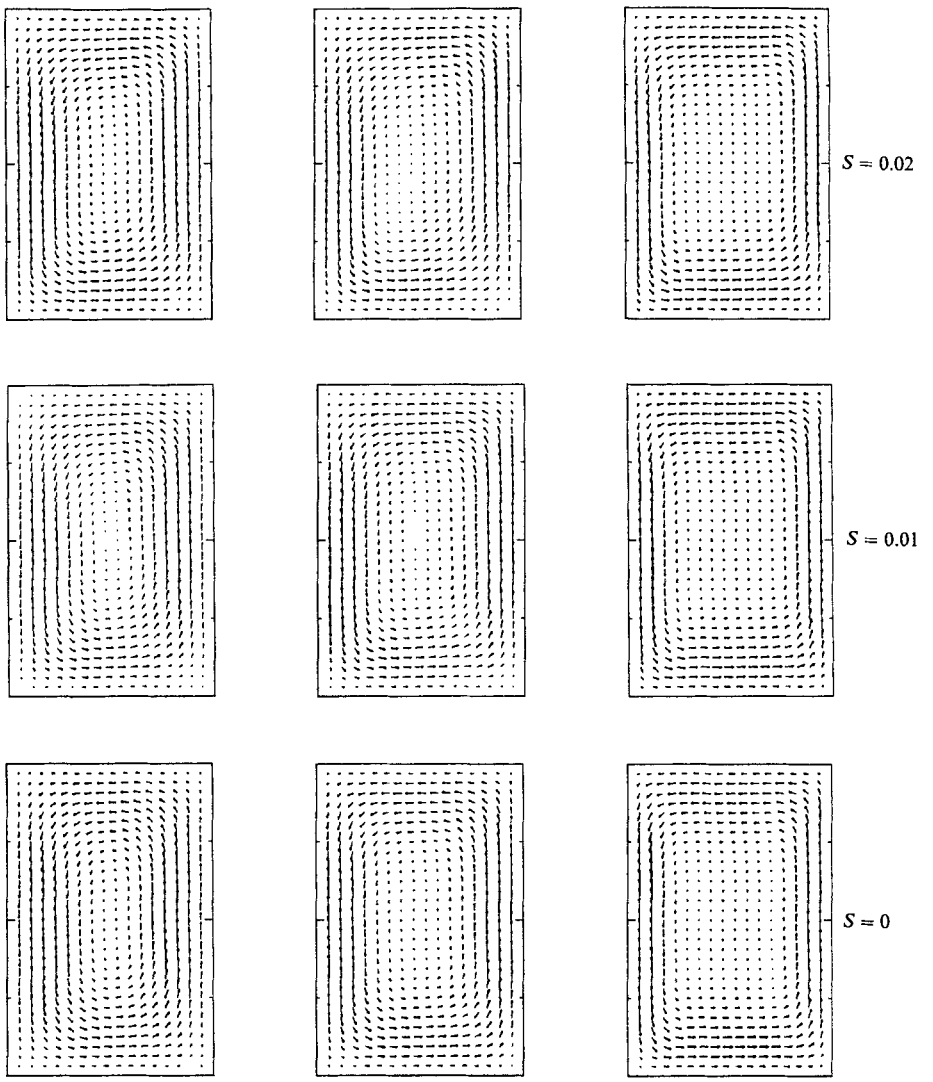

FIGURE 5. Velocity fields in the V-plane, for small Soret parameters ($0 \leqslant S \leqslant 0.02$).

For $S = 0$ and $482 \leqslant Gr \leqslant 4820$, we observe that $\beta_X > 90°$ in the centre. For small but finite S, iso-mass-fraction contours are still strongly distorted and generate a force opposite to F_T (as $\beta_X = 90°$ and $\gamma = 1°$, i.e. $\beta_X > \gamma$), but as S and $(\partial X/\partial n)$ are small, F_X is less than F_T and slightly slows down the motion, which always presents the same structure (with a central region at rest). This leads to a smaller deformation of the X-contours and a better separation rate, but this influence is only significant for very small values of Gr (see figure 7). For high Gr, the separation tends to an asymptotic limit, as shown in figure 10. Such a limit, close to 0.17, is quite similar to the one observed by Henry & Roux (1986) for $\gamma = 90°$ when $Gr \sim 10$.

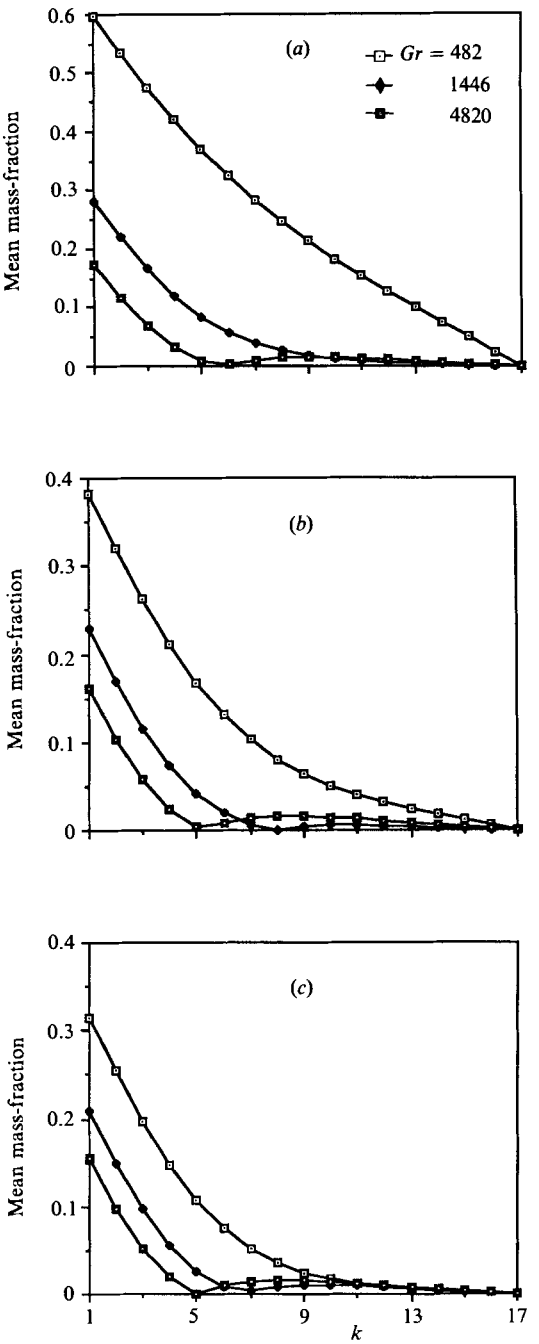

FIGURE 6. Evolution of the mean mass-fraction $|X_m|/(\frac{1}{2}A)$ along the axis (in terms of k), for small Soret parameters: (*a*) $S = 0.02$; (*b*) 0.01; (*c*) 0.

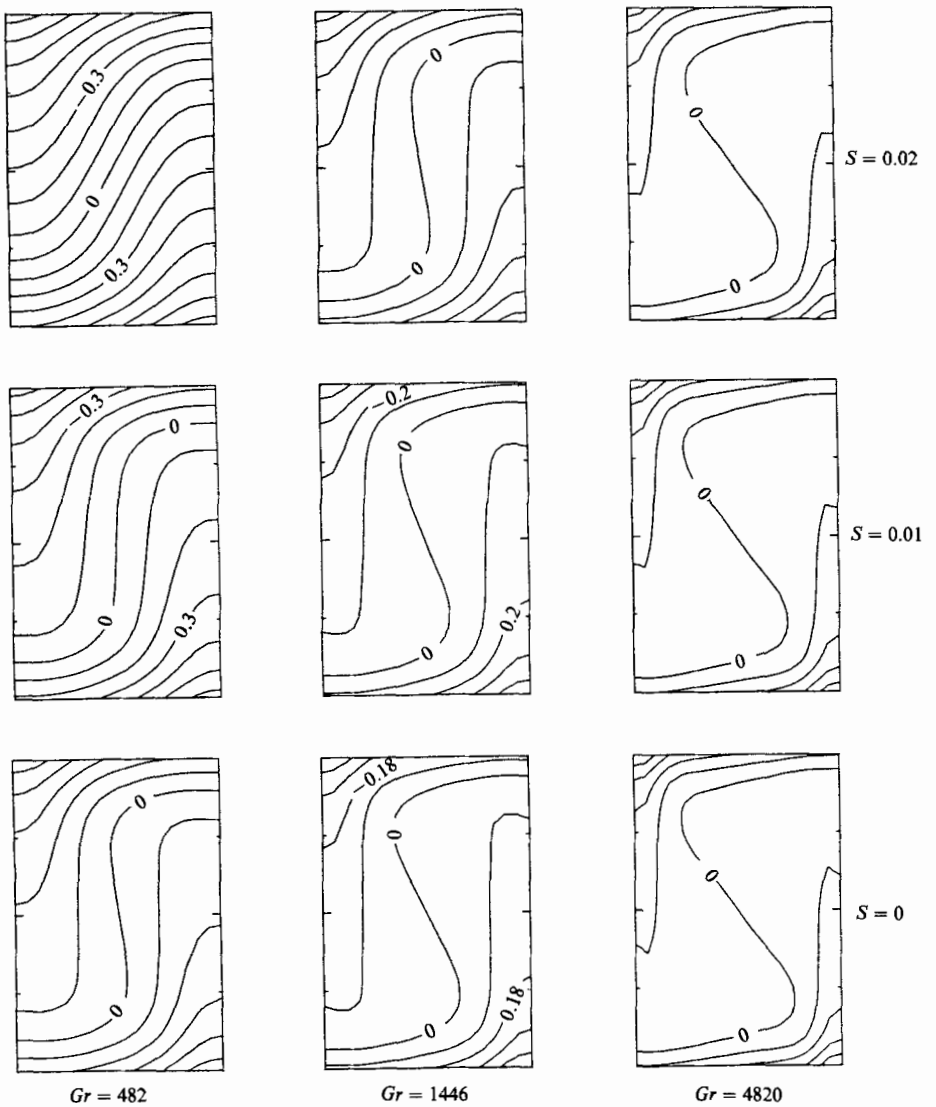

FIGURE 7. Iso-mass-fraction contours for small S: $DX = 0.1$, except at $Gr = 1446$ for $S = 0$ where $DX = 0.09$ and at $Gr = 4820$ where $DX = 0.09$ for $S = 0.02$, $DX = 0.08$ for $S = 0.01$ and $DX = 0.07$ for $S = 0$.

5. Moderate Soret parameter ($0.05 \leqslant S \leqslant 0.673$)

5.1. *General comments*

The velocity fields in the V-plane (see figure 11) present some differences for higher S ($0.05 \leqslant S \leqslant 0.3$), compared to that presented in figure 5 for $0 \leqslant S \leqslant 0.02$, but they all show a central zone at rest. Some particle tracks in the V-plane, given in figure 12 for $S = 0.673$, exhibit again more clearly such a central zone, mainly for high Gr ($Gr = 4820$). For high Gr, figures 11 and 12 also show a recirculating zone (contrarotative rolls) near the two endwalls.

The iso-mass-fraction contours (in figure 13) exhibit a uniform inclination (except near the lateral walls); this structure is quite different from the one (of remixing

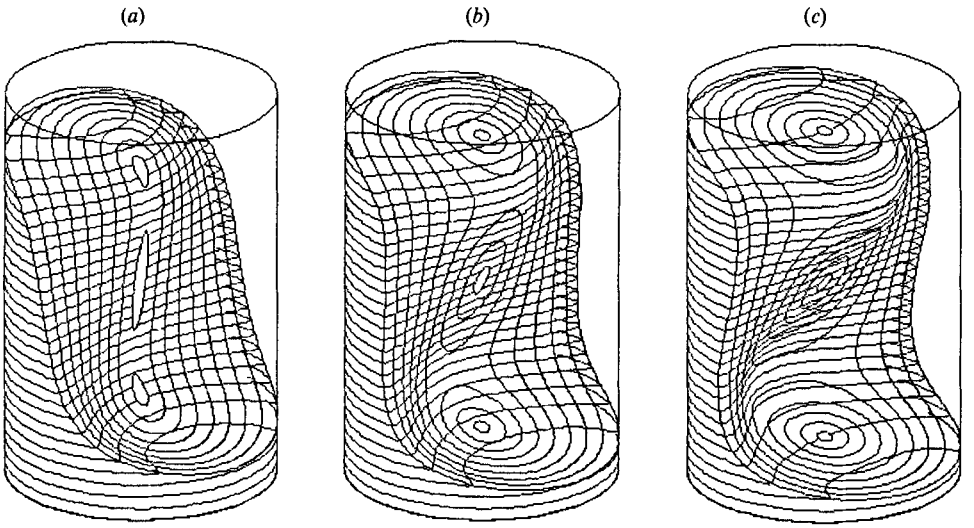

FIGURE 8. Three-dimensional description of the zero-mass-fraction contour at $S = 0$. (a) $Gr = 482$; (b) 1446; (c) 4820.

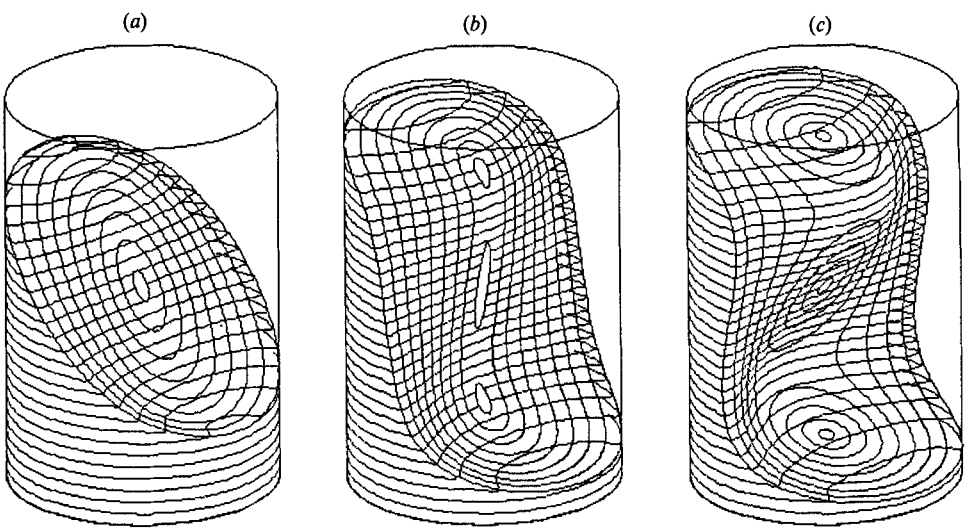

FIGURE 9. Three-dimensional description of the zero-mass-fraction contour at $S = 0.02$. (a) $Gr = 482$; (b) 1446; (c) 4820.

type) observed in figure 7 for low S. The three-dimensional representation of the zero-X contours (figure 14) shows that this characteristic (uniform inclination) is valid for the whole cylinder (except near the lateral walls). In addition, we can see that the value of β_X that corresponds to this inclination decreases when S increases.

In any part of the cylinder the velocity appears to be small compared with that of the case $S = 0$ (purely thermal buoyancy), meaning that F_T is completely neutralized by F_X, whose sign is opposite in any case ($\beta_X > \gamma$). Using (8) and (10), that (mechanical) equilibrium condition can be written as

$$F_T + F_X = \sin(1°) - SX_n \sin(\beta_X - 1°) = 0. \tag{11}$$

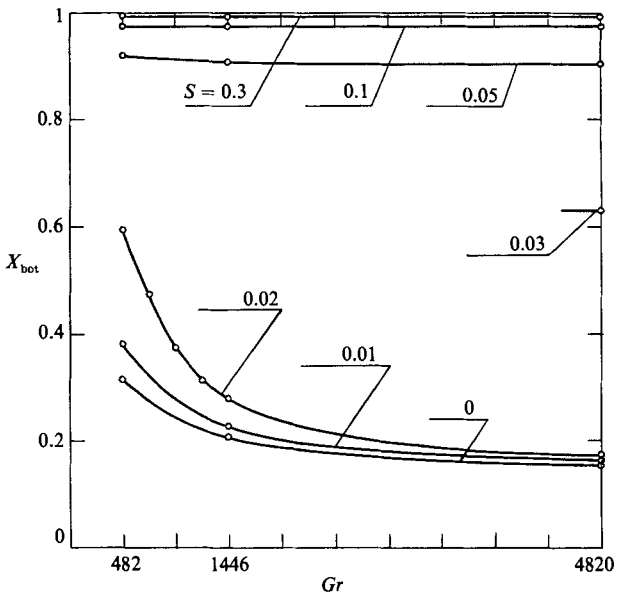

FIGURE 10. Global species separation, X_{bot} *vs.* Gr, for different Soret parameters.

When $X_n \sim 1$, which is true for moderate S, we obtain

$$\beta_X - 1° = \arcsin[\sin(1°)/S] \sim 1°/S. \tag{12}$$

Thus $(\beta_X - 1°)$ which represents the inclination of the iso-mass-fraction contours with respect to the horizontal, on the axis, is inversely proportional to S. To confirm this interpretation, we compare the numerical value of this inclination $(\beta_X - 1°)$ with (12) in table 1. The computed value of $(\beta_X - 1°)$ for $S = 0.03$ is also mentioned in table 1, but in fact (12) does not apply correctly to such a small S. Nevertheless, table 1 shows that β_X increases when S diminishes, and leads to a worse separation rate (X_z or X_n), which in turn requires a higher β_X to reach the equilibrium given by (11). To be more rigorous we would have to take the isotherm deformations, β_T, into account and thus use (9) instead of (10); the equilibrium (11) would be more easily satisfied but qualitatively the result would be the same.

This mechanical equilibrium corresponding to weak flows and inclined mass-fraction field allows good separation rates. The perturbation of the global separation X_{bot} remains small (X_{bot} close to 1) as long as the X-contour inclination is not too great. We can see, in figure 15, that this separation is excellent for $S \geqslant 0.3$. It is still good for $0.1 \leqslant S \leqslant 0.3$ and acceptable for $S = 0.05$. Thus, at $\gamma = 1°$, the limit for performing an accurate measurement of the Soret coefficient would correspond to $S = 0.1$, which leads to a limit value $\beta_X \sim 10°$ for the X-contour inclination.

One could think that the balancing of F_X and F_T given by the condition (11) could make possible an 'overstable' motion such as the one occurring in double-diffusive systems (when the diffusivities are sufficiently different) for cylinders heated from below and negative S (Henry & Roux 1983, see figure 7), and which could correspond to the oscillations reported by Hurle & Jakeman (1973) for slightly inclined (small aspect ratio) cylinders. In fact, such an oscillatory behaviour has never been observed in all the cases considered herein, but we can note that the convergence of numerical solutions is always more difficult to achieve when this balancing occurs

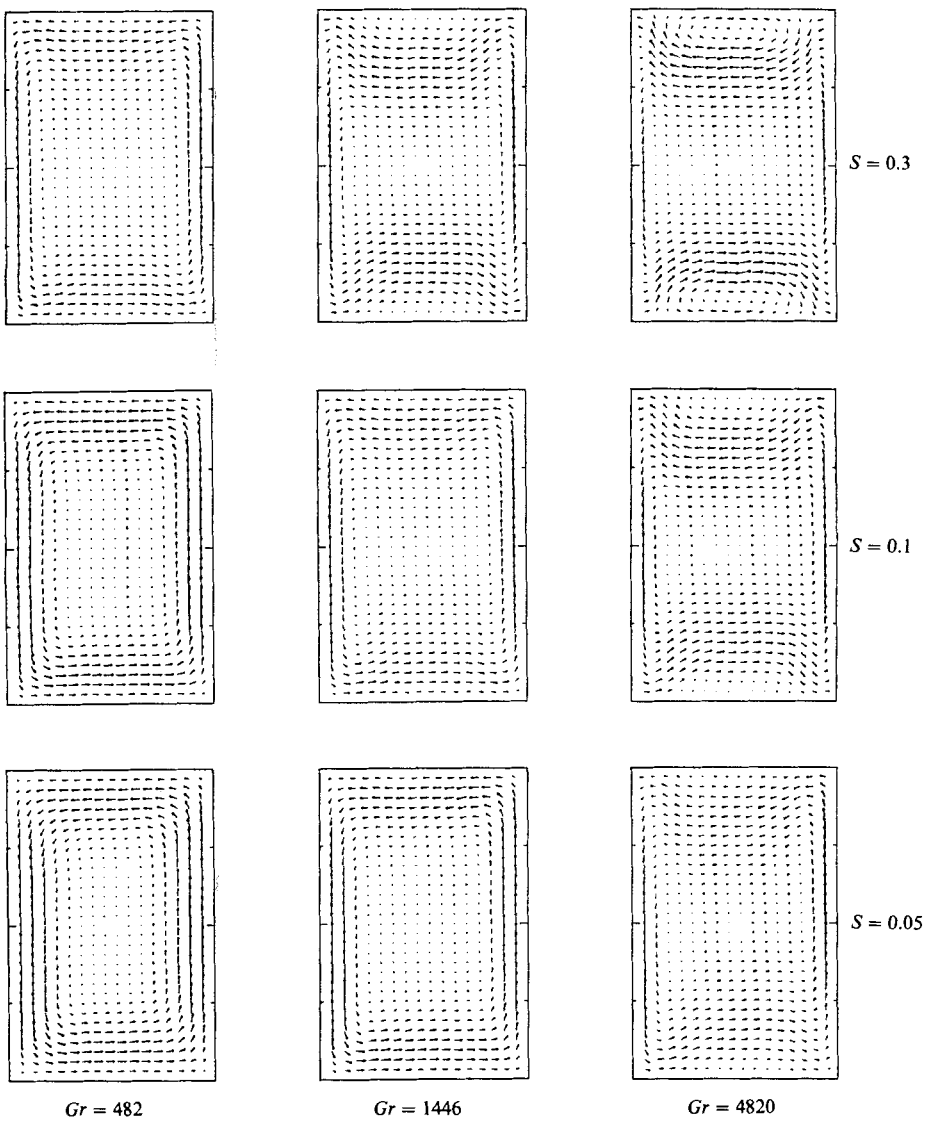

FIGURE 11. Velocity fields in the V-plane, for moderate Soret parameters ($S = 0.05$, 0.1 and 0.3) at various Grashof numbers.

than otherwise (when the driving forces are balanced by the viscous forces). In our system, the flow is generated by solutal and thermal buoyancy forces created by the inclination of the X- and T-fields due to the cell inclination. But a further evolution for both thermal and solutal fields will tend to stabilize the system: the generated flow creates a deformation of the T- and X-fields which in turn generates restoring forces acting in the same direction to slow down this flow or even stop it.

5.2. *Influence of the walls*

In the main part of the cylindrical cell the velocity is small, but as already mentioned a significative flow exists near the walls.

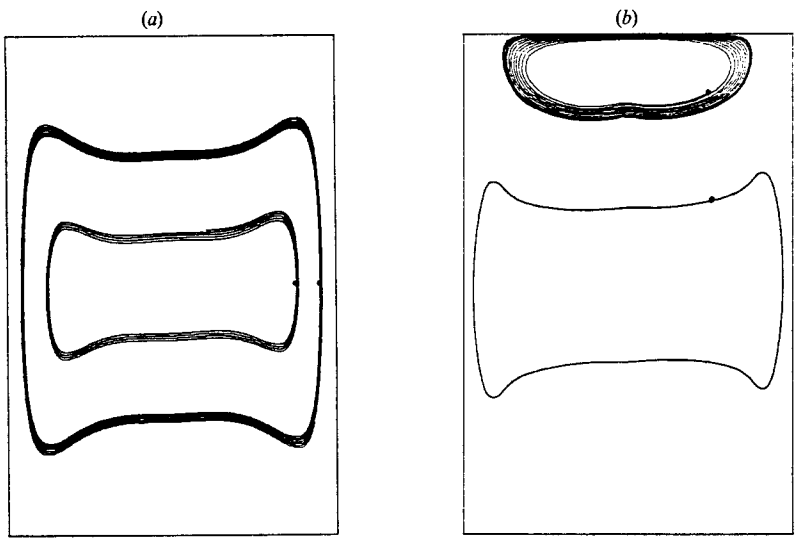

FIGURE 12. Particle tracks in the V-plane at $S = 0.673$. The particles are released at different points (r,z): (*a*) for $Gr = 482$, at $(r = 0.75,\ z = 1.5)$ and $(r = 0.9,\ z = 1.5)$; (*b*) for $Gr = 4820$, at $(r = 0.5,\ z = 1.0)$ and $(r = 0.5,\ z = 0.35)$.

5.2.1. *On the lateral walls*, the no-mass flux condition leads to

$$T_r + X_r = 0. \tag{13}$$

Therefore, as the isotherms are not deviated by the flow ($T_r \sim 0$), the condition (13) gives

$$X_r \sim 0, \tag{14}$$

which means that the iso-mass-fraction contours, perpendicular to the lateral walls, are not deformed by the flow. In particular, in the V-plane, we have $\beta_X = 0°$ ($\beta_X < \gamma$), and then (8) shows that solutal buoyancy, F_X, is smaller than F_T but acts in the same way. Thus a flow is generated in a small layer adjacent to the lateral wall; the thickness of this layer diminishes when S increases (figure 11), because the inclination of the X-contours in the central region needed for the equilibrium (11) is weak. Thus the transition to the 'unperturbed' zone near the lateral wall is rapid. This thickness is also smaller for higher Gr (figure 11). (Equilibrium reached on a larger part of the cell.)

5.2.2. *On the endwalls*, the no-mass flux condition leads to

$$T_z + X_z = 0, \tag{15}$$

and, as the isotherms are not deviated by the flow ($T_z \sim -1$), the condition (15) gives

$$X_z \sim 1. \tag{16}$$

In that case, using (7) and (10), the total buoyancy force can be written as

$$F = F_T + F_X = \sin(1°) + S[\sin(1°) - X_r \cos(1°)]. \tag{17}$$

In our study the solutal and thermal buoyancy forces are often opposite (as $\beta_X > \gamma$), but the thermal contribution generally remains higher. In fact, near the endwalls, we can observe the reverse situation with a (small) contrarotating flow near the endwalls

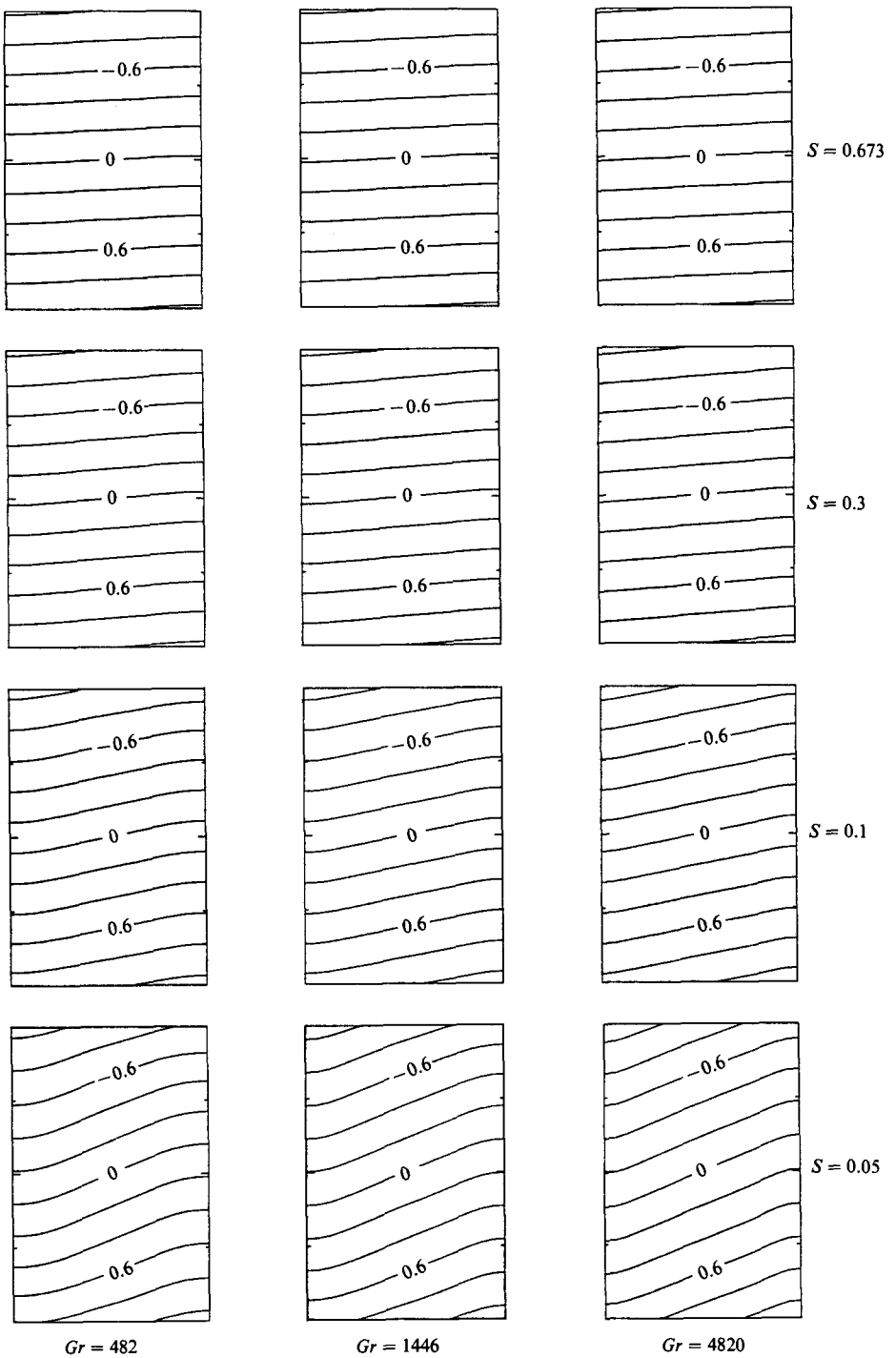

FIGURE 13. Iso-mass-fraction contours for moderate Soret parameters; $DX = 0.2$.

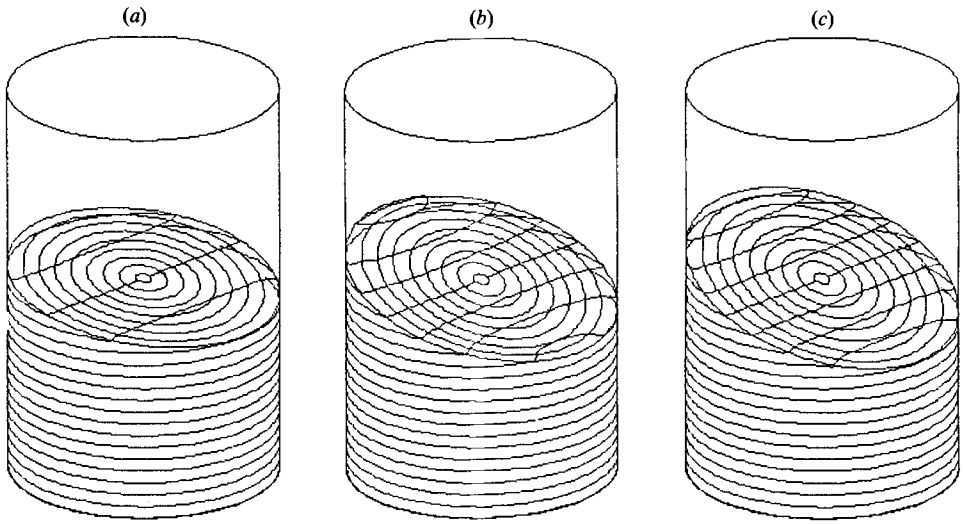

FIGURE 14. Three-dimensional description of the zero-mass-fraction contour: (*a*) $S = 0.1$, $Gr = 4820$; (*b*) $S = 0.05$, $Gr = 482$; (*c*) $S = 0.05$, $Gr = 4820$.

	Gr			
S	482	1446	4820	Equation (12)
0.673	1.5°	1.5°	1.5°	1.5°
0.3	3.3°	3.4°	3.4°	3.3°
0.1	10.2°	10.1°	10.3°	10°
0.05	21.4°	20.9°	21.7°	20°
0.03	—	—	49.4°	33.3°

TABLE 1. Values of $(\beta_X - 1)$ in degrees obtained at different Gr, and from (12)

(F and F_T being of opposite sign). This can be seen for $Gr = 4820$, in figure 11 with $S = 0.3$ and more clearly in figure 12 with $S = 0.673$. This contrarotating flow occurs when $|F_X| > F_T$. The ratio $R_F = |F_X|/F_T$ in the middle of the endwall is given in figure 16 as a function of S for different Gr. The existence of a contrarotative roll in the V-plane is well observed near the endwalls in case when $R_F > 1$; but this condition is not strictly sufficient, the ratio R_F having to be high enough. If R_F is only slightly greater than 1, we observe that the flow slows down only near the endwalls, e.g. for $Gr = 4820$ with $S = 0.1$ and for $Gr = 1446$ with $S = 0.3$. The same behaviour is observed when R_F is slightly smaller than 1, as for $Gr = 1446$ with $S = 0.1$ and for $Gr = 482$ with $S = 0.3$.

For moderate S the flow in a quasi-vertical cylinder is mainly driven near the walls; the same behaviour was observed in the steady basic state of double-diffusive regimes by Paliwal & Chen (1980*b*, figure 2).

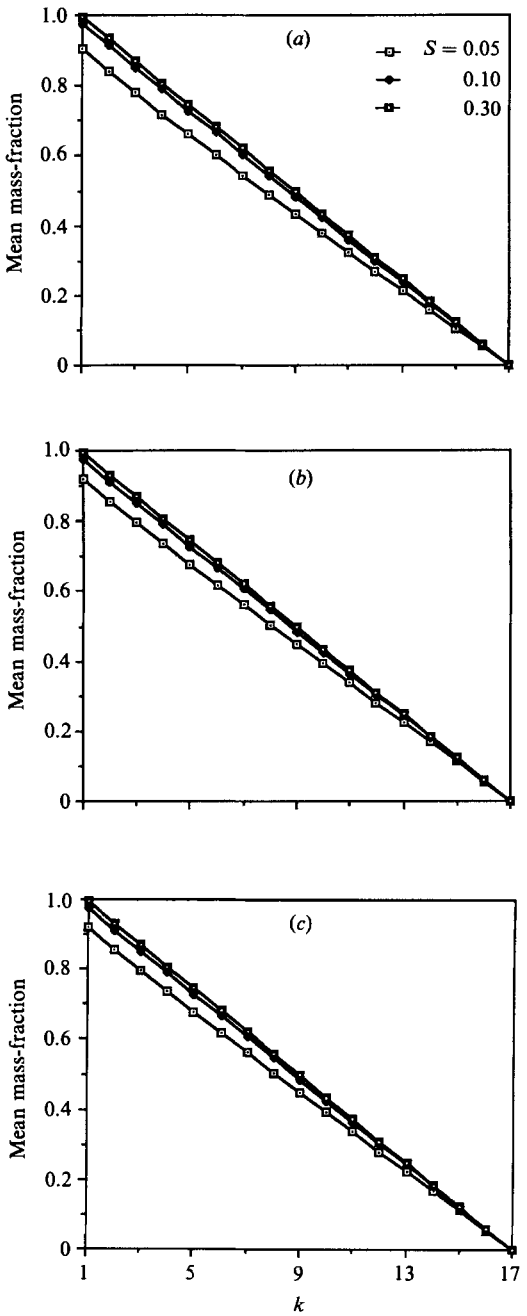

FIGURE 15. Evolution of the mean mass-fraction $|X_m|/(\frac{1}{2}A)$ along the axis (in terms of k), for moderate Soret parameters. (*a*) $Gr = 4820$; (*b*) 1446; (*c*) 482.

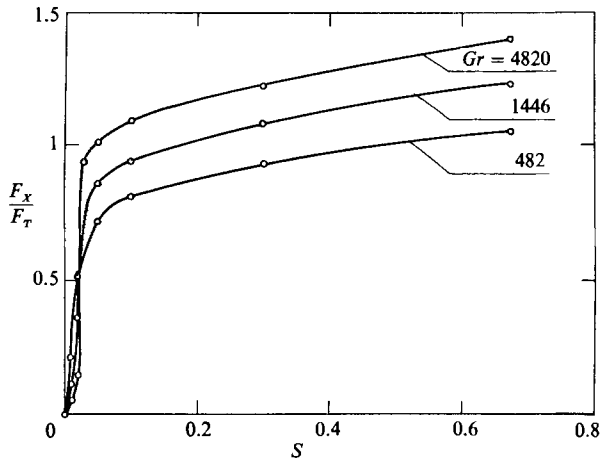

FIGURE 16. Ratio of solutal and thermal buoyancy forces, F_X/F_T, near the endwalls in terms of the Soret parameter, for various Grashof numbers.

6. Transition domain

It is interesting to look at the transition between the two domains described in the previous sections as they exhibit quite different flow behaviours.

Figures 3 and 4 show that the domain of moderate S (for which an equilibrium has been seen to exist in the central region) can also be characterized by $\tilde{V}_{\max}$ and X_{bot} being independent of Gr. We can give a theoretical extreme limit of this domain by considering that F_X cannot exceed the value corresponding to vertical X-contours, i.e. $(\beta_X - 1°) = 90°$. Taking $X_n = 1$, the equilibrium expressed by (11) would then be satisfied when

$$S \geqslant \frac{\sin(1°)}{\sin(90°)} = 0.01745. \tag{18}$$

In fact X_n diminishes with the inclination and $X_n \ll 1$ for $(\beta_X - 1°) = 90°$; thus this limiting value of S is not very accurate but appears qualitatively acceptable.

Another means to estimate the transition domain is to calculate F_X in the centre and to compare it to F_T which is assumed constant and equal to $\sin(1°)$, as in (10). The comparison is given in figure 17 which indicates that an obvious equilibrium is obtained down to $S = 0.05$. Below this value the transition clearly occurs for high Gr ($Gr = 4820$ in the interval $0.02 < S < 0.03$) while it appears smoother for smaller Gr.

This transition can also be seen from a phenomenological point of view. For moderate S, the theoretical inclination β_X given by (12) to reach the equilibrium is weak, X_n is close to 1, and thus (11) is well satisfied. When S diminishes, β_X given by (12) increases, inducing a reduction of X_n. The value needed to reach the equilibrium, which is given in that case by (11), is still higher. In addition, as β_X increases, the thickness of the layer adjacent to the lateral walls increases and the central zone of constant X-contour inclination reduces. As we have seen before, when S is too small ($S < 0.03$) the equilibrium cannot be maintained, except in a very small domain near the centre, owing to a slight deformation of the isotherms.

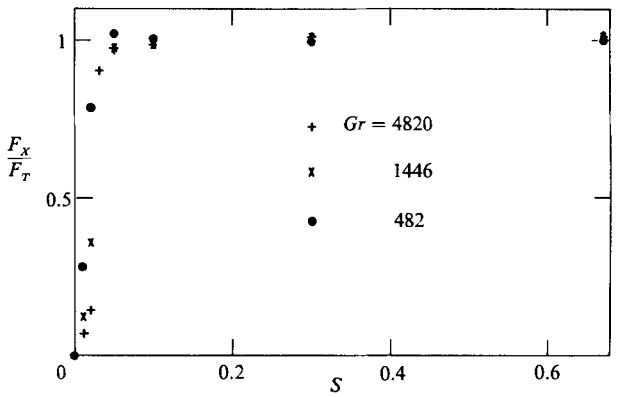

FIGURE 17. Ratio of solutal and thermal buoyancy forces, F_X/F_T, near the centre in terms of the Soret parameter, for various Grashof numbers.

7. Influence of the main parameters

7.1. *Grashof effect*

The influence of Gr, in the range $482 \leqslant Gr \leqslant 4820$ considered herein, is not important. For the high values of Gr, i.e. values inducing a strong deformation ($\beta_X = 90°$) of the zero-X contour in the limit case $S = 0$, the extent of the equilibrium domain will be as mentioned in the previous sections, with quite similar values of S for the transition.

For smaller Gr, the differences observed between the two domains will be less important, as the deformation is smaller for $S = 0$. That confirms previous results obtained by Henry & Roux (1987*a*) for very small Gr ($1 \leqslant Gr \leqslant 3$), for which no transition was observed on the curves X_{bot} versus S (X_{bot} being already close to 1 for $S = 0$). Furthermore, for small enough Gr (as $Gr = 1$) where $\beta_X \sim 0$ (i.e. $\beta_X < \gamma$), F_X has the same sign as F_T and tends to reinforce the motion due to F_T (but this motion remains weak).

Finally, on the domain of moderate S, the separation will be good for any value of Gr. But, for small Gr, such a good separation corresponds to weak F_T and F_X, while for high Gr it corresponds to an equilibrium between opposite values of F_T and F_X.

7.2. *Aspect-ratio effect*

Some numerical simulations which have been done for higher A (namely $A = 6$) show that increasing A does not have a large influence on the behaviours discussed in the previous sections.

For the domain of moderate S, these behaviours are identical (corresponding to an equilibrium between F_T and F_X and leading to an excellent separation ($X_{\text{bot}} = 1$)).

For small S (up to the transition) where a certain longitudinal motion exists, the behaviours are slightly different as the confinement is different, but the main effect of A on X_{bot} is similar to the one discussed in our previous paper for small Gr (Henry & Roux 1986), i.e. X_{bot} diminishes when A increases, for a given Gr.

7.3. *Influence of the cell inclination*

The interpretation of the results for $\gamma = 1°$ can be extended to any (small) value of γ. The expressions (11) and (12) for the equilibrium are easily generalized by

$$F_T + F_X = \sin(\gamma) - SX_n \sin(\beta_X - \gamma) = 0. \tag{19}$$

When $X_n \sim 1$, which is true for moderate S, we obtain

$$\beta_X - \gamma = \arcsin[\sin(\gamma)/S] \sim \gamma/S. \tag{20}$$

Consequently, for any small γ, we shall have the two domains of S mentioned before, but the localization of the transition will depend on γ. We shall mainly consider the equilibrium-state domain (higher S) which gives a good separation.

For a given γ, we can calculate the lower limit value, S_{lim}, of this equilibrium-state domain. We have seen that this limit would correspond to $\beta_X \sim 10°$ and $X_n \sim 1$. According to (20), we have

$$S_{\text{lim}} = \sin(\gamma)/\sin(10° - \gamma). \tag{21}$$

For small γ ($\gamma \leqslant 1°$), (21) gives

$$S_{\text{lim}} \sim \gamma/10°. \tag{22}$$

A good separation is only possible for $S > \gamma/10°$; thus for a smaller S, a smaller value of γ is required.

On the other hand, for higher γ ($1° \leqslant \gamma < 10°$), S_{lim} increases following (21). A sort of limit is exhibited by (21), for $\gamma = 10°$, which indicates that beyond this value (or a value close to 10°) a good separation will be impossible for any S.

It is also interesting to consider the effect of the cell inclination for a given S, and for high Gr. For $\gamma = 0°$, the separation is perfect for any $S \geqslant 0$ (stable stratification). As soon as γ increases, F_T becomes significant and generates a motion. In the case where the solutal effect is uncoupled ($S = 0$), this motion is strong (for high Gr) and leads to a strong deformation of the X-contours. If $S \neq 0$, the solutal coupling slows down this motion and thus, for S not too small, an equilibrium can be reached in a certain domain of γ, $0 \leqslant \gamma \leqslant \gamma_{\text{lim}}$. This limit cell inclination, γ_{lim}, is small for small S and will increase with S, but it cannot exceed 10°. In conclusion, it will only be possible to obtain a good separation, for high Gr, on a smaller and smaller interval ($0 \leqslant \gamma \leqslant \gamma_{\text{lim}}$) when S decreases.

7.4. *Comments on the cases of negative S*

We did not systematically consider the case of negative S; but we can given some general comments for that case. A first difference from the case of positive Soret effect, shown by the linear stability study previously done (Henry & Roux 1983), is that a critical value of Gr for the onset of convection at $\gamma = 0°$ exists. (Gr_c is decreasing with S.) But, results presented in a previous paper by Henry & Roux (1987*b*) for supercritical Gr (see their figure 5) show that the concentration fields at $\gamma = 1°$ and $\gamma = 0°$ are about the same, even for slightly supercritical Gr. Additional computations carried out for a highly supercritical Gr ($Gr = 482$) at $S = -0.1$ (for which Gr_c is close to 20) and $\gamma = 1°$ give $X_{\text{bot}} = 0.208$ (to be compared to $X_{\text{bot}} = 0.315$ at $S = 0$, in figure 4). Thus, it is easy to imagine that the graphs of figures 3 and 4 would simply correspond, for negative S, to a smooth continuation of the one calculated for positive S.

In fact, in the previous study (Henry & Roux 1987*b*), we have shown that for $Gr < 1.33$, no instability occurs at $\gamma = 0°$, and for any $\gamma \neq 0°$ a positive S increases the flow. In these cases the separation at $\gamma = 1°$ is good for any S ($S > -1$).

For larger Gr, there is a negative critical S ($-1 < S_c < 0$) beyond which an instability occurs at $\gamma = 0°$, and, at least in the vicinity of $\gamma = 0°$, a positive S decreases the flow. In that case, the bifurcation obtained at $\gamma = 0°$ for S_c (sudden decrease of X_{bot}) will give with $\gamma = 1°$ a smoother imperfect bifurcation beginning for values of S slightly higher than S_c. For small Gr, as $Gr = 3$ ($S_c = -0.45$), this

imperfect bifurcation begins for negative values of S and then does not affect the values of X_{bot} for $S > 0$. But for larger Gr (corresponding to small $|S_c|$) as $Gr \geqslant 482$, this imperfect bifurcation begins or even occurs mainly in the domain of positive S, giving the observed variations drawn in figure 4.

Finally, with $\gamma = 1°$, except for very small Gr ($Gr \leqslant 1.33$), the separation for negative S (for given Gr, Pr, Sc and A) will be worse than for the case $S = 0$ (this corresponds to the evolution of the imperfect bifurcation). With $\gamma = 0°$, the separation is perfect down to the (negative) critical S, and decreases quickly afterwards: a good approximation is then given for such situations (not too close to the critical one) by the corresponding results with $\gamma = 1°$.

7.5. *Other comments*

We wish now to answer an interesting question of one of the reviewers about the possible occurrence of layering regimes which correspond to a double-diffusive instability of stationary type occurring in a stably stratified fluid layer subjected to lateral temperature gradient. This layering phenomenon was reported for example by Thorpe, Hutt & Soulsby (1969), Hart (1971, 1973), Turner & Chen (1974), Huppert & Turner (1981). It has been emphasized by Paliwal & Chen (1980*a*, *b*) in two companion papers covering experimental and theoretical (stability analysis) approaches in the case of an inclined fluid layer confined within two parallel walls; they specially considered the limit case of a vertical fluid layer subjected to a horizontal temperature gradient. A condition for the layering occurrence is that a steady basic state (with density-stratified fluid) should exist prior to the onset of instabilities. We have seen in §§5.1 and 7.3 that, for inclined cylinders with Soret effect, this condition is only satisfied for small cell inclinations, γ, when S is not too small; i.e. when $S > S_{\text{lim}}$, where S_{lim} is given by (22) (for large aspect ratios ($A \geqslant 3$), the limit value of S is $S_{\text{lim}} = 6\gamma$, with γ expressed in radians). In such cases, the values of the thermal and solutal Rayleigh numbers, according to the definitions given by Paliwal & Chen (1980*b*), can be expressed as $R_T = 16 Gr\, Pr \sin\gamma$ (based on the destabilizing horizontal component of the temperature gradient) and $R_S = 16 Gr\, Pr\, S \cos\gamma$.

Then, in our case, a condition for the layering occurrence is

$$R_S > 6R_T, \tag{23}$$

and thus the instability condition derived by Paliwal & Chen (1980*b*) for a vertical fluid layer subjected to a horizontal temperature gradient, which corresponds to a curve slightly below the first diagonal in the range $10^2 \leqslant R_S \leqslant 10^5$ (see figure 5 of Paliwal & Chen 1980*b*), is never satisfied. (See also figure 3 of Hart 1971.)

Furthermore we can see that for an initially given (stable) solutal stratification the layering is generally obtained by varying (increasing) independently the lateral thermal gradient. In our case, the increase of $\Delta T'$ (which generally allows the instability to be reached) increases R_T, but also R_S by the same factor (due to the Soret effect) and thus in the stability diagram of Paliwal & Chen (1980*b*, figure 5) the functional curve (R_T, R_S) would almost be parallel to the threshold stability line without crossing it. We can also note that in our case we have a vertical component of the temperature gradient which is stabilizing and still reinforces the role of R_S. We therefore conclude that layering regimes are not to be expected in the case of long cylindrical cells with Soret effect.

8. Comparison with previous results and discussion

We can compare our results to those of Dulieu *et al.* (1981) who carried out a two-dimensional numerical study of the convection in a parallelepipedic cell heated from the top and subjected to a small inclination. They linearized the governing equations with respect to the inclination angle, γ, and solved this simplified problem by using a Galerkin method. They obtained an estimation of the Soret coefficient, D'/D, that could be observed. This value $(D'/D)_{\text{obs}}$ is smaller than the one corresponding to a perfect separation without convection, the reduction being expressed as a quadratic function of the perturbation parameter:

$$\frac{(D'/D)_{\text{obs}}}{(D'/D)} = 1 - \alpha_s \left[\frac{(1+S)\,Sc}{Pr}\right]^2 \gamma^2, \tag{24}$$

where α_s is a function of the parameters Ra, k and α defined as

$$Ra = \frac{\alpha g L^3 (\bar{T}_{\text{h}} - \bar{T}_{\text{c}})}{16 \nu \kappa}, \quad k = A^{-1}, \quad \alpha = S\,Sc/Pr.$$

The ratio (24) is similar to X_{bot} in our computations. For a given Ra ($Ra = 8000$), Dulieu *et al.* (1981) give the variation of α_s in terms of α for various aspect ratios, $0.1 \leqslant k \leqslant 10$. Their figure 2 exhibits two domains in α (similar to our two domains in S) with a transition zone between $\alpha = 1$ and $\alpha = 10$; α_s is less than 10^{-2} for $\alpha > 10$. For $\alpha = 10$, which corresponds to $S = 0.1$ for $Sc/Pr = 100$ (a quite general value for liquids), the expression (24) gives a relative difference for the Soret parameter close to 4%, for an inclination $\gamma = 1°$. This result well agrees with the limiting value $S = 0.1$ given by (22) with $\gamma = 1°$; in that case $X_{\text{bot}} = 0.975$ (i.e. the separation is only 2.5% smaller than the perfect one). For high confinement (for example $k = 0.1$), their α_s remains small (for any α) indicating small remixing; this is not in contradiction with our results as their parameter values ($Ra = 8000$ and $k = 0.1$) correspond, in our study, to a small value of Gr ($Gr = 21$ at $A = 10$) leading to an unperturbed situation for any S.

Dulieu *et al.* (1981) also give variations of α_s in terms of Ra, for $\alpha = 0$ and $\alpha = 0.1$, showing an increase of α_s with Ra, but with a tendency to reach a limiting value for high Ra (see their figure 4). These curves can be compared to our results giving X_{bot} in terms of Gr, for different S, in figure 10; an increase of α_s corresponds to a diminution of X_{bot}, as shown by the expression (24).

We can also comment the comparisons done by Dulieu *et al.* (1981) with the results obtained by Agar & Turner (1960).

(*a*) We agree with the stabilizing effect of increasing α (or $S\,Sc/Pr$), but we can add some precision, pointing out that the restabilizing solutal buoyancy forces are proportional to the product $Gr\,S\,Sc$. For small S, where the equilibrium does not exist (except in the centre), the iso-mass-fraction deformation and X_{bot} will depend on Sc. But for moderate S, where the equilibrium is reached in almost the entire cylinder, the values of Sc (as soon as they are strong enough to permit a strong deformation of the concentration field) will not influence the results which will mainly depend on S.

(*b*) Dulieu *et al.* (1981) mention that for given α and k, an increase of Ra does not favour the separation. In fact this is true for small S, while for higher S (where an equilibrium can be reached) an increase of Gr (or Ra) slightly strengthens the motion but does not significantly change the value of X_{bot}.

(c) Agar & Turner (1960) indicate that the influence of the convection has to be correlated to Sc/Pr and to $Ra_T + Ra_S = 16Ra(1+\alpha)$. Dulieu *et al.* (1981) agree on the role of α, but not on that of Ra. In fact, Agar & Turner (1960) considered the case of a strictly vertical cell (originally subjected to a strictly vertical temperature gradient) at which they applied, at $t = 0$, a temperature alteration able to generate horizontal components of both thermal and solutal gradients. Both these gradients will tend to re-establish the initial equilibrium, after some delay, by generating a motion. Using $Gr_D = Ra/Pr$ and considering that $T_r \sim Pr$ and $X_r \sim Sc$, the strength of this 'restoring' motion can be expressed in the V-plane (containing the main flow due to disturbances), as

$$V \sim Gr_D(T_r + SX_r) \sim Gr_D(Pr + S\,Sc) = Ra(1+\alpha). \tag{25}$$

Thus, in the case of a strictly vertical cylinder as considered by Agar & Turner (1960), the velocity of the flow which tends to restabilize the system is closely proportional to Ra. The stronger Ra is the sooner the strictly vertical gradients will be restored. This is a fundamental difference with the case of a quasi-vertical cell where a horizontal temperature gradient is maintained and where the solutal gradient only is able to restabilize the system.

9. Conclusion

We have studied the Soret separation in a differentially heated cylinder. As soon as such a cylinder is slightly inclined, at a small angle γ, the mixture inside is subjected to the thermal buoyancy which generates a flow. For the case considered herein (elongated cylinder ($A = 3$), moderate Prandtl number ($Pr = 0.6$), high Schmidt number ($Sc = 60$) and positive S), this flow does not distort the temperature profiles except for the small values of S combined with high values of Gr. In these last cases, the isotherm deformation remains weak ($\beta_T \sim 1°$), but it can considerably modify the thermal buoyancy forces, F_T, mainly in the centre where the motion may be vanishing. In the other cases (small Gr or moderate S) when the isotherms are not distorted, we have $F_T = \sin\gamma$.

If the iso-mass-fraction deformation, β_X, is weak and smaller than γ, which is the case for small Gr, the mass-fraction reinforces the flow but this flow remains weak and the separation is still very good. If $\beta_X \geqslant \gamma$ (for higher Gr), the roles of X and T are opposite: the solutal buoyancy tends to slow down the motion. In fact, for moderate S, the solutal buoyancy is strong enough to balance the driving thermal buoyancy and to create a rest state in most of the cell, providing a good separation. On the other hand, for small S, the solutal buoyancy does not permit such a rest state to be reached (except in the centre); it only slows down the motion and does not prevent poor separation, for high Gr. Finally, the smaller the Soret coefficient is, the smaller the inclination defect γ has to be to allow a good separation rate.

In addition, our results in a quasi-vertical cylinder show that a mixture corresponding to high Sc (liquid metals, molten salts, etc.) and particularly a mixture corresponding to low Pr (liquid metals) could present strong concentration inhomogeneities, in the vertical direction, due to the thermal (Soret) diffusion and in the radial direction due to the thermally driven convection induced by even a small geometrical defect in the heating system. This point could be of interest in crystal growth or solidification techniques like the 'vertical Bridgman', as it indicates the possible occurrence of a radial macrosegregation near the solidification front.

The authors thank the Centre National d'Etudes Spatiales (Division Microgravité Fondamentale et Appliquée) for giving financial support, and the Centre de Calcul Vectoriel pour la Recherche for providing them with computing time on the Cray-1S computer. They warmly acknowledge Professor R. Sani for fruitful discussions and reviewers for pertinent remarks and suggestions.

REFERENCES

ABERNATHEY, J. R. & ROSENBERGER, F. 1981 Soret diffusion and convective stability in a closed vertical cylinder. *Phys. Fluids* **24**, 377–381.

AGAR, J. N. & TURNER, J. C. R. 1960 Thermal diffusion in solutions of electrolytes. *Proc. R. Soc. Lond.* A **255**, 307–330.

BERT, J., HENRY, D., LAYANI, P., CHUZEVILLE, G., DUPUY, J. & ROUX, B. 1984 Space experiment on thermal diffusion–preparation and theoretical analysis. In *Proc. Fifth European Symposium on Material Sciences under Microgravity* (ESA SP-222), pp. 347–351. ESA Publ. Division c/o ESTEC, Noordwijk, The Netherlands.

BERT, J. MOUSSA, I. & DUPUY, J. 1987 Space thermal diffusion experiment in a molten AgI–KI mixture. In *Proc. Sixth European Symposium on Material Sciences under Microgravity* (ESA SP-256), pp. 471–475. ESA Publ. Division c/o ESTEC, Noordwijk, The Netherlands.

CALDWELL, D. R. 1973 Measurement of negative thermal diffusion coefficients by observing the onset of thermohaline convection. *J. Phys. Chem.* **77**, 2004–2008.

CHIEN, C. P. & MATTES, B. L. 1983 Thermal Soret diffusion in the liquid phase epitaxial growth of binary III–V compounds. *J. Vac. Sci. Technol.* B *Microelec. Proc. and Phen.* **1**, 648–655.

CHOCK, D. P. & LI, C. H. 1975 Direct integration method applied to Soret-driven instability. *Phys. Fluids* **18**, 1401–1406.

CRESPO, E. & VELARDE, M. G. 1982 Two component-Bénard convection in cylinders. *Intl J. Heat Mass Transfer* **25**, 1451–1456.

DE GROOT, S. R. 1947 *L'effet Soret*. North-Holland.

DULIEU, B., CHANU, J. & WALCH, J. P. 1981 A propos de l'influence de la convection sur la mesure de l'effet Soret: le cas d'un défaut d'horizontalité. *J. Chim. Phys.* **78**, 193–201.

GUTKOWICZ-KRUSIN, D., COLLINS, M. A. & ROSS, J. 1979 Rayleigh–Bénard instability in nonreactive binary fluids. II. Results. *Phys. Fluids* **22**, 1451–1460.

HARDIN, G. R., SANI, R. L., HENRY, D. & ROUX, B. 1988 Buoyancy driven instability in a vertical cylinder: Binary fluid with Soret effect. Part 1. General theory and stationary stability results. *Intl J. Num. Math Fluids.* (submitted).

HARP, E. J. & HURLE, D. J. T. 1968 *Phil. Mag.* **17**, 1033.

HART, J. E. 1971 On sideways diffusive instability. *J. Fluid Mech.* **49**, 279–288.

HART, J. E. 1973 Finite amplitude sideways diffusive instability. *J. Fluid Mech.* **59**, 47–64.

HENRY D. 1986 Simulation numérique 3D des mouvements de convection thermosolutale d'un mélange binaire – étude paramétrique de l'influence de la convection sur la séparation des espèces du mélange, par effet Soret, dans un cylindre incliné. Thèse de Doctorat d'Etat, Université Claude Bernard Lyon I.

HENRY, D. & ROUX, B. 1983 Stationary and oscillatory instabilities for mixture subjected to Soret effect in vertical cylinder with axial temperature gradient. In *Proc. Fourth European Symposium on Material Sciences under Microgravity* (ESA SP-191), pp. 145–152. ESA Publ. Division c/o ESTEC, Noordwijk, The Netherlands.

HENRY, D. & ROUX, B. 1986 Three-dimensional numerical study of convection in a cylindrical thermal diffusion cell: its influence on the separation of constituents. *Phys. Fluids* **29**, 3562–3572.

HENRY, D. & ROUX, B. 1987*a* Three-dimensional numerical study of convection in a cylindrical thermal diffusion cell: inclination effect. *Phys. Fluids* **30**, 1656–1666.

HENRY, D. & ROUX, B. 1987*b* Numerical study of the perturbation of Soret experiments by 3D buoyancy driven flows. In *Proc. Sixth European Symposium on Material Sciences under Microgravity* (ESA SP-256), pp. 487–491. ESA Publ. Division c/o ESTEC, Noordwijk, The Netherlands.

HUPPERT, H. E. & TURNER, J. S. 1981 Double-diffusive convection. *J. Fluid Mech.* **106**, 299–329.

HURLE, D. T. J. & JAKEMAN E. 1969 Significance of the Soret effect in the Rayleigh–Jeffreys' problem. *Phys. Fluids* **12**, 2704–2705.

HURLE, D. T. J. & JAKEMAN, E. 1971 Soret-driven thermosolutal convection. *J. Fluid Mech.* **47**, 667–688.

HURLE, D. T. J. & JAKEMAN, E. 1973 Thermal oscillations in convecting fluids. *Phys. Fluids* **16**, 2056–2059.

LEGROS, J. C., VAN HOOK, W. A. & THOMAES, G. 1968 Convection and thermal diffusion in a solution heated from below. *Chem. Phys. Lett.* **2**, 249–250.

LEGROS, J. C., RASSE, D. & THOMAES, G. 1970 Convection and thermal diffusion in a solution heated from below. *Chem. Phys. Lett.* **4**, 1383–1385.

LEONG, S. S. & DE VAHL DAVIS, G. 1979 Natural convection in a horizontal cylinder. In *Proc. First Intl Conf. on Numerical Methods in Thermal Problems, University College, Swansea*, pp. 287–296. Pineridge.

LONGREE, D., LEGROS, J. C. & THOMAES, G. 1980 Measured Soret coefficients for simple liquified gas mixture at low temperatures. *J. Phys. Chem.* **84**, 3480–3483.

MALMEJAC, Y. & PRAIZEY, J. P. 1984 Thermomigration of cobalt in liquid tin. In *Proc. Fifth European Symposium on Material Sciences under Microgravity* (ESA SP-222), pp. 147–152. ESA Publ. Division c/o ESTEC, Noordwijk, The Netherlands.

OLSON, J. M. & ROSENBERGER, F. 1979 Convective instabilities in a closed vertical cylinder heated from below. Part 2. Binary gas mixtures. *J. Fluid Mech.* **92**, 631–642.

PALIWAL, R. C. & CHEN, C. F. 1980*a* Double-diffusive instability in an inclined fluid layer. Part 1. Experimental investigation. *J. Fluid Mech.* **98**, 755–768.

PALIWAL, R. C. & CHEN, C. F. 1980*b* Double-diffusive instability in an inclined fluid layer. Part 2. Stability analysis. *J. Fluid Mech.* **98**, 769–785.

PLATTEN, J. K. & CHAVEPEYER, G. 1972 Soret driven instability. *Phys. Fluids* **15**, 1555–1557.

PLATTEN, J. K. & CHAVEPEYER, G. 1976 Instabilité et flux de chaleur dans le problème de Bénard à deux constituants aux coefficients de Soret positifs. *Intl J. Heat Mass Transfer* **19**, 27–32.

PLATTEN, J. K. & CHAVEPEYER, G. 1977 Nonlinear two dimensional Bénard convection with Soret effect: free boundaries. *Intl J. Heat Mass Transfer* **20**, 113–122.

PLATTEN, J. K. & LEGROS, J. C. 1984 *Convection in Liquids*, pp. 650–652. Springer.

PRAIZEY, J. P. 1987 Results of the D1-WL-GHF-07 thermomigration in metallic alloys. In *Sixth European Symposium on Material Sciences under Microgravity* (ESA SP-256), pp. 501–508. ESA Publ. Division c/o ESTEC, Noordwijk, The Netherlands.

SCHECHTER, R. S., PRIGOGINE, I. & HAMM, J. R. 1972 Thermal diffusion and convective stability. *Phys. Fluids* **15**, 379–386.

SCHECHTER, R. S., VELARDE, M. G. & PLATTEN, J. K. 1974 The two-component Bénard problem. *Adv. Chem. Phys.* **26**, 265–301.

SHIRTCLIFFE, T. G. L. 1969 An experimental investigation of thermosolutal convection at marginal stability. *J. Fluid Mech.* **35**, 677–688.

SMUTEK, C., ROUX, B., BONTOUX, P. & DE VAHL DAVIS, G. 1984 3D finite difference for natural convection in cylinders. In *Proc. Fifth Gesellschaft für Angewandte Mathematik und Mechanik-Conference*. Notes on Numerical Fluid Mechanics, vol. 7, pp. 338–345. Vieweg.

SUNDHEIM, B. R. & KELLNER, J. D. 1965 Thermoelectric properties of the molten silver nitrate–sodium nitrate system. *J. Phys. Chem.* **69**, 1204–1208.

THOMAES, G. 1975 The Bénard instability in liquid mixtures. *Adv. Chem. Phys.* **32**, 269–279.

THORPE, S. A., HUTT, P. K. & SOULSBY, R. 1969 The effect of horizontal gradients on thermohaline convection. *J. Fluid Mech.* **38**, 375–400.

TURNER, J. S. & CHEN, C. F. 1974 Two-dimensional effects in double-diffusive convection. *J. Fluid Mech.* **63**, 577–592.

VELARDE, M. G. & SCHECHTER, R. S. 1971 Thermal diffusion and convective stability: a critical survey of Soret coefficient measurements. *Chem. Phys. Lett.* **12**, 312–315.

VERHOEVEN, J. D. 1969 Experimental study of thermal convection in a vertical cylinder of mercury heated from below. *Phys. Fluids* **12**, 1733–1740.